

Military Technical College,  
Kobry El-Kobbah,  
Cairo, Egypt



9<sup>th</sup> International Conference  
On Aerospace Sciences &  
Aviation Technology

## OPTIMUM SLOT SIZE AND LOCATION IN A RADIAL VANE IMPELLER FOR BETTER CENTRIFUGAL PUMP PERFORMANCE

M.S.E.Hussien\*, A.H.Lotfy\*, H.M.Abdalla\*, I.Saleh\*

### ABSTRACT

The centrifugal pump performance depends to great extent upon the flow pattern in the impeller passages. When the pump operates at small flow rates, the problem of circulation due to vortex formation in the impeller passages is found. A new method is introduced to control and reduce the size of generated vortices in the impeller passages. Slots are opened in the impeller vanes to allow fluid to flow from the pressure side to the suction side of the vane. The bleeding fluid could reduce the size of the vortices. It is found to depend mainly upon the length and the position of the slot. In the present work, the flow field is solved in the radial impeller passages using the stream function and the primitive variable approaches, to solve the flow equations. The flow pattern is used to compare the vortex size and the pump head for both cases with and without slotted impeller vanes at different slot sizes and at different positions. The slot position that produces the highest pump head, the slot length has been changed until the smallest vortex size is achieved. The numerical solution is introduced in a code program form, which is written in the *Microsoft Visual C++ 6* language. Finally the optimum position and length of the slot is obtained at  $R_s/R_2 = 0.4981$ , and with  $L/(R_2-R_1) = 0.2291$ . The model has been validated by comparison to a published experimental result of the same pump (for the same research program).

### KEY WORDS

Flow Pattern, Vortex, Turbomachinery, Impeller, Computational Fluid Dynamics, Centrifugal Pump.

---

\*Egyptian Armed Forces.

**NOMENCLATURE**

B	Impeller width.	(m)
$\mu$	Dynamic viscosity.	(kg/m. s)
$\nu$	Kinematics viscosity = $\mu / \rho$ .	(m <sup>2</sup> /s)
Bt	Blade thickness.	(m)
C	Average radial component of absolute velocity.	(m/s)
CS	Begin of slot	(m)
e	Unit vector in polar coordinate system.	
E, F	Flux vector.	
F <sub>t</sub>	Time factor.	
g	Gravity acceleration.	(m/s <sup>2</sup> )
H	Pump head.	(m)
i	Node index (step level) in radial direction.	
j	Node index (step level) in tangential direction.	
L	Slot length.	(m)
M	Number of grids in tangential direction; integer number (M=1,2,..j).	
n	Impeller rotational speed.	(r.p.m)
N	number of grids in radial direction; integer number(N = 1,2,...i).	
p	Static pressure.	(Pa)
Q	Conservation variable; Flow rate.	(m <sup>3</sup> /s)
Q <sub>n</sub>	Nominal flow rate.	(m <sup>3</sup> /s)
r	Radial coordinate.	
Rs	Slot pitch radius.	(m)
S	Arc length.	(m)
t	Time.	(s)
U <sub>r</sub>	Relative radial component flow velocity.	(m/s)
U <sub>o</sub>	Relative tangential component flow velocity.	(m/s)
Z	Number of impeller blades.	
$\delta$	Artificial factor.	
$\theta$	Tangential coordinate.	
$\rho$	Fluid density.	(kg/m <sup>3</sup> )
$\omega$	Impeller angular velocity.	(s <sup>-1</sup> )

**Superscripts**

- Predictor.
- ~ Artificial value.
- n Refer to time level (step).

**INTRODUCTION**

The flow field inside the impeller passages may be described by the continuity and Navier-stokes equations. Present methods for solving these equations consists of: solving equations of motion in the primitive parameters (velocities and pressure), or by using vorticity and stream function approach. Solution using the first approach has been reported by many investigators [1,2,3,4,5]. Different numerical methods have been used in solving these equations in differential form. The main disadvantage of

these numerical methods lies in the need of considerable computation time and difficult treatment of boundary conditions.

### FLOW FIELD ANALYSIS

For vaned impeller, having inner diameter  $D_1$ , outer diameter  $D_2$  and number of vanes  $Z$ , the present work presents the development of a steady two-dimensional, incompressible Navier-Stokes equations, solved in a polar-coordinate system using primitive variables. The method is applied to a centrifugal pump of radial blades. The difficulty in calculating the flow pattern may be simplified after making the following assumptions:

1. Neglecting the turbulence effect.
2. Incompressible and steady flow.
3. The impeller is assumed to rotate in an infinite field.
4. Smooth change in flow from axial to radial direction in the impeller inlet section.
5. The width of the impeller passage is constant.
6. Two-dimensional flow (neglecting the 3-D effect on velocity).
7. The flow enters the impeller passages tangent to the blade.

### GOVERNING EQUATIONS

Consider the polar-coordinate system  $(r, \theta)$  illustrated in Fig. (1), where  $r$  denotes the radial coordinate and  $\theta$  denotes the tangential coordinate. The governing equations are written in **primitive-variable form**, where  $p, u_r, u_\theta$  are the **primitive-variables**; (Hirsch C), [6].

#### Continuity

$$\frac{\partial \rho}{\partial t} + \frac{\rho}{r} \frac{\partial}{\partial r}(ru_r) + \frac{\rho}{r} \frac{\partial}{\partial \theta}(u_\theta) = 0 \quad (1)$$

#### Momentum

From assumptions, the turbulent shear stresses will be neglected, but the gradient of viscous term ( $\mu \nabla^2 u$ ) becomes important in the boundary-layer regions.

$$\frac{\partial}{\partial t}(u_r) + \frac{1}{r} \frac{\partial}{\partial r}(ru_r^2) + \frac{1}{r} \frac{\partial}{\partial \theta}(u_r u_\theta) - \frac{u_\theta^2}{r} - r\omega^2 - 2\omega u_\theta = -\frac{1}{\rho} \frac{\partial p}{\partial r} + \nu \left[ \nabla^2 u_r - \frac{u_r}{r^2} - \frac{2}{r^2} \frac{\partial u_\theta}{\partial \theta} \right] \quad (2)$$

$$\frac{\partial}{\partial t}(u_\theta) + \frac{1}{r} \frac{\partial}{\partial \theta}(ru_r u_\theta) + \frac{1}{r} \frac{\partial}{\partial \theta}(u_\theta^2) + \frac{u_r u_\theta}{r} + 2\omega u_r = -\frac{1}{\rho r} \frac{\partial p}{\partial \theta} + \nu \left[ \nabla^2 u_\theta - \frac{u_\theta}{r^2} + \frac{2}{r^2} \frac{\partial u_r}{\partial \theta} \right] \quad (3)$$

$$\nabla^2(\ ) = \frac{\partial^2}{\partial r^2}(\ ) + \frac{1}{r} \frac{\partial}{\partial r}(\ ) + \frac{1}{r^2} \frac{\partial^2}{\partial \theta^2}(\ ) \quad (\text{For polar coordinates})$$

The artificial density is related to the pressure by the artificial equation of state:

$$p = \delta \tilde{\rho} \quad (4)$$

Using equation (1) and (4) the following form is obtained:

$$-\frac{\partial}{\partial t}(p) = \rho \delta \left[ \frac{1}{r} \frac{\partial}{\partial r}(ru_r) + \frac{1}{r} \frac{\partial}{\partial \theta}(u_\theta) \right] \quad (5)$$

## FLOW FIELD

The impeller vanes are of radial type with constant width. The following assumptions are taken for the geometry of blade and slot:

- The blade thickness is not constant (increases in radial direction).
- The blade slot passage is a part of radial concentric circles.

These are shown in Fig. (1).

The computational domain is discretized into mesh points. The present scheme calculates the flow through one blade passage. The computational boundaries comprise the upstream inlet, the downstream exit, and the pressure and suction sides of blade surface. Logically, polar grid is used in the present method.

Uniform radial concentric circles and radial rays divide the blade passage, as shown in Fig. (1), and form the grid or nodes.

- a) Radial concentric circles apart by constant intervals ( $\Delta r$ ):

$$\Delta r = \frac{R_2 - R_1}{(N - 1)} \quad (6)$$

- b) Inter vanes sections, apart by arc length ( $S_i$ ) at circle  $i$

$$S_i = r_i \Delta \theta \quad (7)$$

$$\Delta \theta = \frac{360}{Z(M - 1)} \quad (8)$$

The most appropriate system of equations in differential form is the Reynolds averaged Navier-Stokes equations in a rotating polar-coordinate system; [7]

$$\frac{\partial Q}{\partial t} + \frac{1}{r} \frac{\partial(rE)}{\partial r} + \frac{1}{r} \frac{\partial F}{\partial \theta} = \frac{1}{r} S + \text{ViscousTerms} \quad (9)$$

Considering equation (9) without viscous terms:

$$\frac{\partial Q}{\partial t} = -\frac{1}{r} \frac{\partial(rE)}{\partial r} - \frac{1}{r} \frac{\partial F}{\partial \theta} + \frac{1}{r} S \quad (10)$$

Using Equations,(2,3,5) we get:

$$Q = \begin{bmatrix} p \\ u_r \\ u_\theta \end{bmatrix} \quad (11)$$

$$E = \begin{bmatrix} \rho \delta u_r \\ u_r^2 + \frac{p}{\rho} \\ u_r u_\theta \end{bmatrix} \quad (12)$$

$$F = \begin{bmatrix} \rho \delta u_\theta \\ u_r u_\theta \\ u_\theta^2 + \frac{p}{\rho} \end{bmatrix} \quad (13)$$

$$S = \begin{bmatrix} 0 \\ u_\theta^2 + p / \rho + \omega^2 r^2 + 2\omega r u_\theta \\ -u_r u_\theta - 2\omega r u_r \end{bmatrix} \quad (14)$$

Predictor-Corrector method proposed by MacCormack; [1] is used to solve the flow field. This method is a two-step procedure based on the Lax-Wendroff scheme, and is widely used for both internal and external flows. This method has second-order accuracy in time and space. It can be used for both steady and unsteady compressible flow, as well as viscous and inviscid flows. For the inviscid flow, in the procedure suggested by MacCormack, an iterative approach and intermediate value  $\bar{Q}_{i,j}^{n+1}$  is obtained by a predictor step, and  $Q_{i,j}^{n+1}$  is obtained by a corrector step, where n is the time step and n+1 is the next one.

The predictor step written for the 2D inviscid equations in polar  $(r, \theta)$  system is given by:

$$\bar{Q}_{i,j}^{n+1} = Q_{i,j}^n - \frac{\Delta t}{r_i \Delta r} [r_{i+1} E_{i+1,j}^n - r_i E_{i,j}^n] - \frac{\Delta t}{r_i \Delta \theta} [F_{i,j+1}^n - F_{i,j}^n] + \frac{S_{i,j} \Delta t}{r_i} \quad (15)$$

It should be emphasized here that this step provides only an approximate value for  $Q_{i,j}^{n+1}$ , and this can be corrected or updated using the following corrector step:

$$Q_{i,j}^{n+1} = \frac{1}{2} \left\{ Q_{i,j}^n + \bar{Q}_{i,j}^{n+1} - \frac{\Delta t}{r_i \Delta r} [r_i \bar{E}_{i,j}^{n+1} - r_{i-1} \bar{E}_{i-1,j}^{n+1}] - \frac{\Delta t}{r_i \Delta \theta} [\bar{F}_{i,j}^{n+1} - \bar{F}_{i,j-1}^{n+1}] + \frac{S_{i,j} \Delta t}{r_i} \right\} \quad (16)$$

The viscous term will be used as central difference form in r and  $\theta$  directions Fig. (2)

The forward and backward differencing can be alternated between predictor and corrector steps as well as between the two spatial derivatives in a sequential fashion. For algorithms of the present type, it is often necessary to add smoothing terms in order to suppress high frequency oscillations. This can easily be accomplished by adding a fourth-order explicit dissipation term to the primitive variables in the two-directions of flow  $(r, \theta)$  for interior points.

$$-\varepsilon_e \left[ (\Delta r)^4 \frac{\partial^4}{\partial r^4} (Q) + (\Delta \theta)^4 \frac{\partial^4}{\partial \theta^4} (Q) \right] \quad (17)$$

Where:  $\varepsilon_e$  is the explicit smoothing coefficient.

Since this is a fourth-order term it does not affect the formal accuracy of the algorithm. The negative sign is required in order to produce positive damping. The smoothing coefficient  $\varepsilon_e$  should be less than approximately  $\frac{1}{16}$  for stability

(Anderson), [1]. A value of 0.05 is used in the present work. The fourth-derivative terms are evaluated using the following finite-difference approximations

$$(\Delta r)^4 \frac{\partial^4}{\partial r^4} (Q_{i,j}) \cong Q_{i+2,j} - 4Q_{i+1,j} + 6Q_{i,j} - 4Q_{i-1,j} + Q_{i-2,j} \quad (18)$$

$$(\Delta \theta)^4 \frac{\partial^4}{\partial \theta^4} (Q_{i,j}) \cong Q_{i,j+2} - 4Q_{i,j+1} + 6Q_{i,j} - 4Q_{i,j-1} + Q_{i,j-2} \quad (19)$$

But at the boundary the second order term is used.

#### STABILITY CONDITION AND CONVERGENCE CRITERIA

The value of the time step  $\Delta t$  necessary to maintain stability is calculated from empirical equation; (Abdalla), [8].

$$\Delta t = \left( \frac{2F_t}{\frac{|u_r|}{\Delta r} + \frac{|u_\theta|}{r\Delta\theta} + 4v \left( \frac{1}{(\Delta r)^2} + \frac{1}{(r\Delta\theta)^2} \right) + \sqrt{\left( \frac{u_r}{\Delta r} + \frac{u_\theta}{r\Delta\theta} \right)^2 + 4\delta \left( \frac{1}{(\Delta r)^2} + \frac{1}{(r\Delta\theta)^2} \right)}} \right) \quad (20)$$

Where,  $F_t$  is the time factor. It is found from experience that the time factor up to 0.9 can be used. In case of an unstable solution, the time factor is reduced by 0.1. The computation solution is converged when the root mean square of the residual in the velocity component  $U_r$  drops below  $10^{-6}$ .

$$RMS = \sqrt{\frac{\sum_{i=1}^{N_i-1} \sum_{j=1}^{M_j} |u_{r,i,j}^{n+1} - u_{r,i,j}^n|^2}{N_i * M_j}} \quad (21)$$

### INITIAL CONDITIONS

The description of the flow for all grid points by relatively real values is one of the most important tasks. This initial guess could be completely arbitrary. This procedure has no effect on the final solution, but it affects the number of iterations needed for solution convergence (time requirement).

Two methods are used for initial conditions. The first method, radial velocity is obtained from the flow rate and geometry of the impeller. Tangential velocity is taken zeros except at the impeller inlet; it is taken from the stream function approach solution. The pressure is considered constant at the outlet, but the pressure of interior and inlet points are estimated by using Bernoulli's constant. At the second method, the values of the velocities and pressure are taken from the stream function approach solution. But the pressure at the outlet is changed to constant value and velocities at the blade surface are considered zeros in case of viscous flow. [9,10]. This method decreases the running time

### BOUNDARY CONDITIONS

The boundary conditions are very important tasks to get the solution.

The velocities at the blade surface are taken zeros due to no slip condition, but at the slot we use the periodicity. The pressure at the blade is calculated from interpolation of the two inside points

In upstream direction, the radial velocity is obtained from flow rate. Tangential velocity is considered as in initial conditions. The pressure is estimated from Bernoulli's constant that is calculated at the points of second row.

In downstream direction, the pressure is considered the same as in initial conditions. The tangential velocity is interpolated from the two inside points, and the radial velocity is calculated from the continuity equation.

### THEORETICAL CHARACTERISTICS OF THE PUMP

The theoretical head of the pump at steady conditions is determined from the obtained results of the flow field at different positions and lengths of the blade slot. The pumping head is calculated as follows:

$$H = \frac{P_2 - P_1}{\rho g} + \frac{C_2^2 - C_1^2}{2g} \quad (22)$$

### COMPUTER CODE

The developed program is written in the *Microsoft Visual C++ 6* language with high number of statements. This program solves the flow in the passage of a radial

impeller by using the stream function as initial approach to the Navier-Stokes equations and taking results for plotting by the help of *Matlab* 5.3.

## RESULTS AND DISCUSSION

The developed computer program has been used to solve the flow field in an impeller of dimensions,  $R_{LE}=0.026$  m,  $R_{TE}=0.0775$  m, number of blades  $Z=6$ , blade width  $B=0.01$ m, blade thickness  $Bt=0.005375$  m, and at different positions and lengths of the blade slot. Water has been used as a working fluid, with pump speed  $n=1500$  r.p.m.

The flow rate is introduced as input data in ( $m^3/s$ ) or in the form of a ratio of the nominal flow rate. The nominal flow rate is determined by the program, where it is the definition of the nominal flow rate is that flow at which no vortex appears in the blade impeller passages. In other words, it is the flow rate at which no negative radial velocity (back flow) appears at the suction side of impeller blade.

At part loads, a vortex is formed in impeller passages at the suction side of the blade due to back flow. In the present work the flow rate is chosen half of the nominal flow rate (i.e.  $Q = 0.5Q_n$ ) to observe the vortex size.

Results are summarized from Fig (3) to Fig (12), as follows:

Fig. (3) and Fig (4) show the flow pattern in normal impeller passage without slots in its blades by using the stream function approach of inviscid flow and primitive-variable approach of viscous flow respectively. Velocities and pressure are calculated from stream function approach and are taken as initial conditions to the primitive-variable approach to reduce the computation time. Fig (4) shows the formed vortex at the suction side of the vane. The calculated pumping head of normal impeller was  $H=8.9934$  m.

From Fig (5) to Fig (9) the flow pattern is solved for slotted impeller at different positions and at fixed length ( $L=0.01$  m) of the slot. These figures show that there are change in the size and location of the formed vortex and of the slip factor, which affects the pumping head. The pumping head is tabulated in table (1) and shown in From that table the optimum position of the slot is  $R_s/R_2= 0.51$ , which gives the maximum pumping head. The effect of changing of the slot length at the position of maximum pumping head at the optimum length of slot is at  $L/(R_2-R_1)=0.2$ . Fig (13,14) shows pumping head for different positions and lengths of slot to insure that is the optimum location and length of the slot, which is given the same rustles.

Hence, the optimum slot size and location for better centrifugal pump performance are at  $R_s/R_2 = 0.52$ , and  $L/(R_2-R_1)= 0.2$  as shown in figures (13,14). In these figures the first point in the left is the pumping head of normal impeller (without slots in its blades).



## CONCLUSION

The opening of a slot in the impeller blades at a certain position and with a certain length affects the pump performance. The best performance is reached at an optimum position of slot at  $R_s/R_2 = 0.52$ , and length  $L/(R_2-R_1) = 0.2$ . Where the pressure fluctuation parameters are reduced compared with the case of blades without slots. Consequently the noise during pump operation is reduced in case of impeller with slotted vanes (Ahmed), [10].

## REFERENCES

1. Anderson D.A., (1984), Tannehill J.C., and Pletcher R.H., "Computational Fluid Mechanics and Heat Transfer", McGraw Hill Book Company, Second Edition.
2. Pozikidis C., (1997), "Introduction to Theoretical and Computational Fluid Dynamics", University Press, Oxford.
3. Bansod P., and Rhie C.M., (1990), "Computation of Flow Through a Centrifugal Impeller with Tip Leakage", AIAA/SAE/ASME/ASSEE 26<sup>th</sup> Joint Propulsion Conference.
4. Barrere M., et al., (1960), Rocket Propulsion, Elsevier Publishing Company.
5. Rizzi A., and Eriksson L.E., (1985), "Computational of inviscid Incompressible Flow with Rotation", Journal of Fluid Mechanics, Vol. 153, pp.275-312.
6. Hirsch C., and Warzee G., (1976), "A Finite-Element Method for Through Flow Calculations in Turbomachines", Transactions of the ASME, Journal of Fluids Engineering, pp. 403-410.
7. Lakshminarayana B., (1991), "An Assessment of Computational Fluid Dynamic Techniques in the Analysis and Design of Turbomachinery – The 1990 Freeman Scholar Lecture", Transactions of the ASME, Journal of Fluids Engineering, Vol.113, pp. 315-352.
8. Abdalla H., (1981), "A Theoretical and Experimental Investigation of the Regenerative Pump with Aerofoil Blades", Ph.D. Thesis, The Royal Military College of Science.
9. Lotfy, A.H., (1981), "Pressure Fluctuations in Radial flow Centrifugal Pumps at Part Loads", M.Sc. Thesis, M.T.C..
10. Ahmed E.A., (1995), "Study of Flow Field in a Radial Vaned Impeller of a Centrifugal Pump and its Effect on Pump Performance", M.Sc. Thesis, M.T.C..

Table1. Pumping head at different slot sizes and different positions.

0.0052	0.0294	0.03	0.10	0.41	7.3015
0.0052	0.0380	0.04	0.10	0.52	7.7978
0.0052	0.0483	0.05	0.10	0.66	7.5976
0.0052	0.0586	0.06	0.10	0.79	7.1839
0.0052	0.0706	0.07	0.10	0.94	7.3156
0.0103	0.0294	0.03	0.20	0.45	7.8403
0.0103	0.0346	0.04	0.20	0.51	10.0067
0.0103	0.0449	0.05	0.20	0.65	8.4688
0.0103	0.0552	0.06	0.20	0.78	6.7460
0.0103	0.0655	0.07	0.20	0.91	6.3055
0.0155	0.0294	0.037	0.30	0.48	8.7205
0.0155	0.0329	0.04	0.30	0.52	9.4170
0.0155	0.0432	0.05	0.30	0.66	9.2025
0.0155	0.0518	0.06	0.30	0.77	7.5985
0.0155	0.0603	0.07	0.30	0.88	5.2709
0.0189	0.0294	0.04	0.37	0.50	8.2559
0.0189	0.0397	0.05	0.37	0.63	9.3942
0.0189	0.0500	0.06	0.37	0.77	6.3787
0.0189	0.0569	0.07	0.37	0.86	4.8051

Note:

- $H=8.9934$  m for radial impeller without slot.
- $Q=0.5Q_n=0.0081045$  m<sup>3</sup>/s.

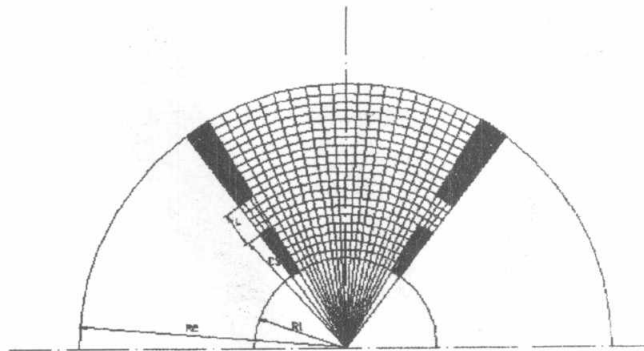


Fig.1. The Blade Profile.

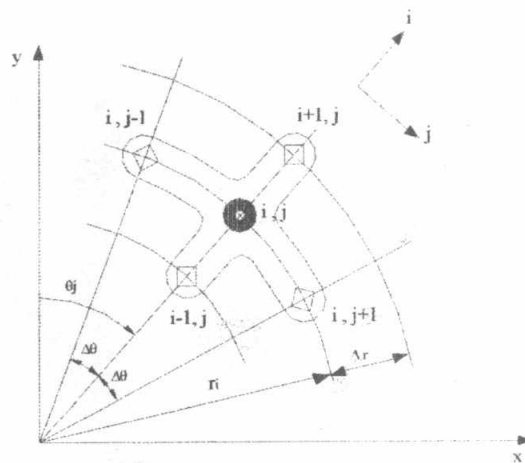


Fig.2. The polar mesh.

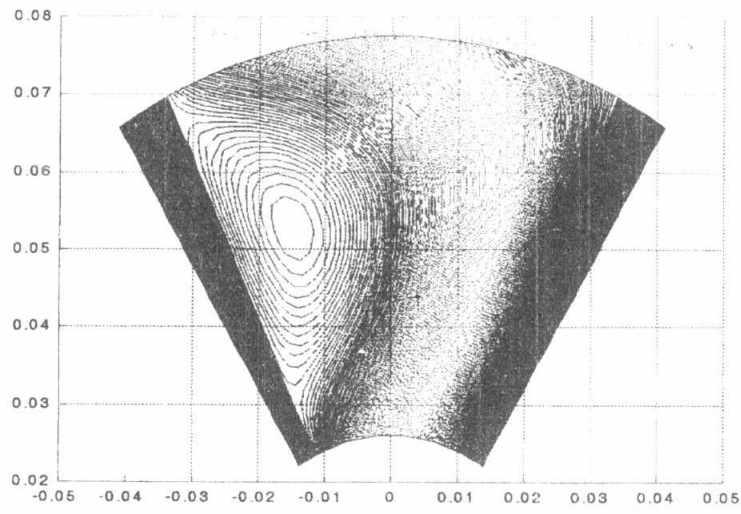


Fig.3. Streamlines of the normal impeller using stream function approach.  
( $Q=0.5Q_n=0.008104 \text{ m}^3/\text{s}$ )

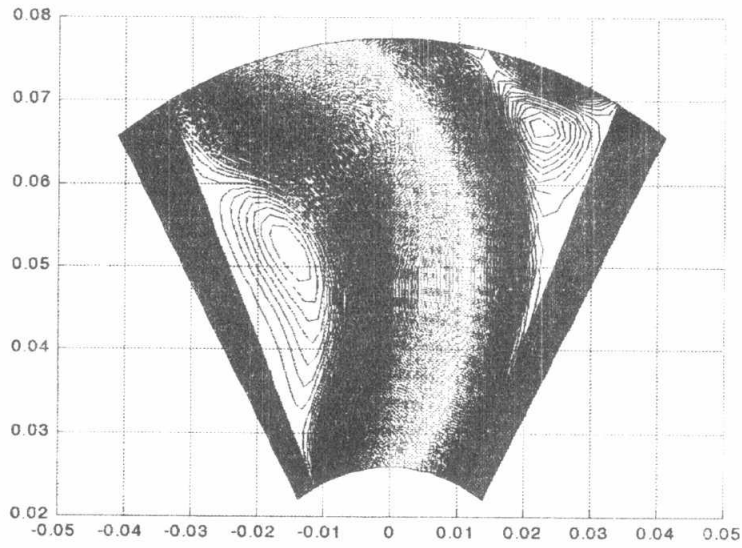


Fig.4. Streamlines of the normal impeller using primitive variables approach.  
( $Q=0.5Q_n=0.008104 \text{ m}^3/\text{s}$ )

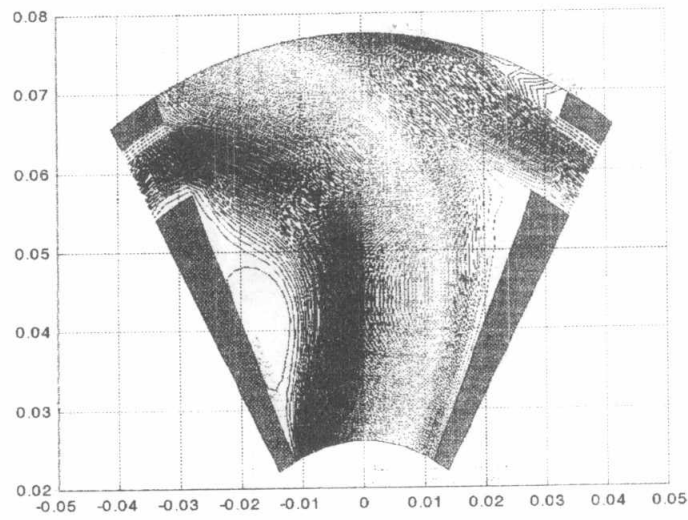


Fig.5. Streamlines of the slotted impeller using primitive variables approach.  
( $Q=0.5Q_n=0.008104 \text{ m}^3/\text{s}$ ,  $L=0.01\text{m}$ ,  $R_s=0.07\text{m}$ , and  $H=6.3055\text{m}$ )

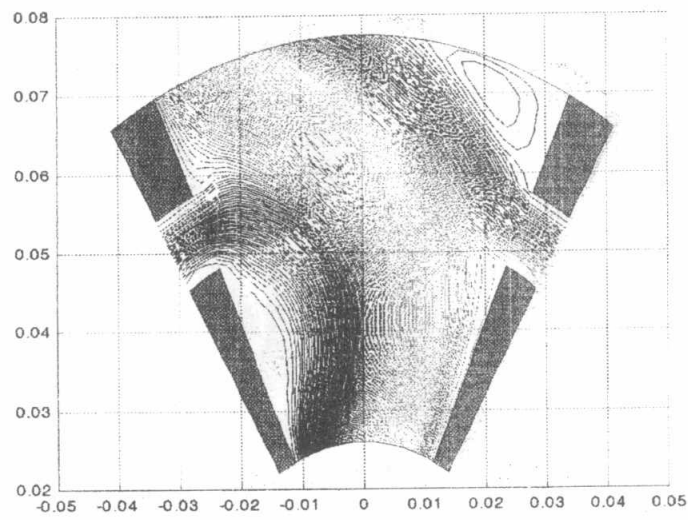


Fig.6. Streamlines of the slotted impeller using primitive variables approach.  
( $Q=0.5Q_n=0.008104 \text{ m}^3/\text{s}$ ,  $L=0.01\text{m}$ ,  $R_s=0.06\text{m}$ , and  $H=6.746\text{m}$ )

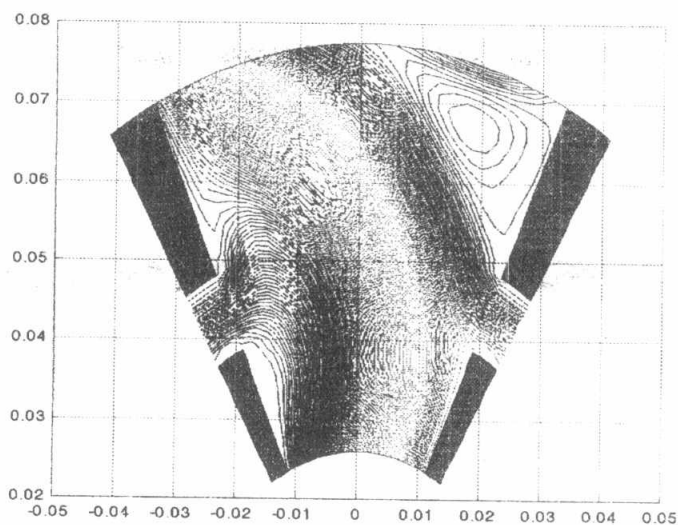


Fig.7. Streamlines of the slotted impeller using primitive variables approach.  
( $Q=0.5Q_n=0.008104 \text{ m}^3/\text{s}$ ,  $L=0.01\text{m}$ ,  $R_s=0.05\text{m}$ , and  $H=8.4688\text{m}$ )

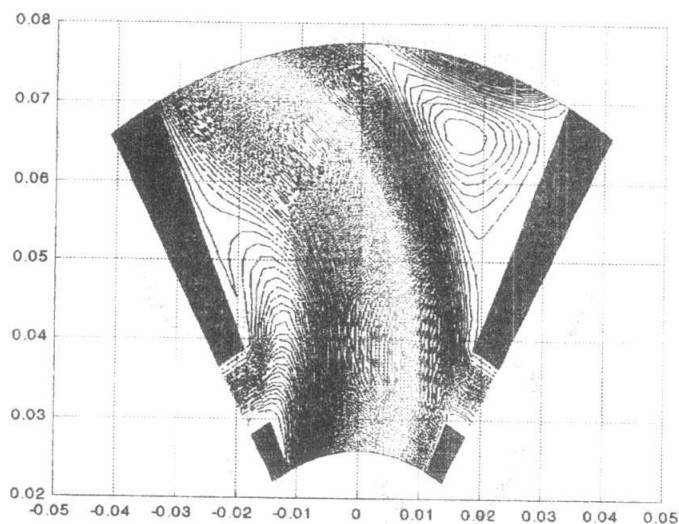


Fig.8. Streamlines of the slotted impeller using primitive variables approach.  
( $Q=0.5Q_n=0.008104 \text{ m}^3/\text{s}$ ,  $L=0.01\text{m}$ ,  $R_s=0.04\text{m}$ , and  $H=10.0067\text{m}$ )

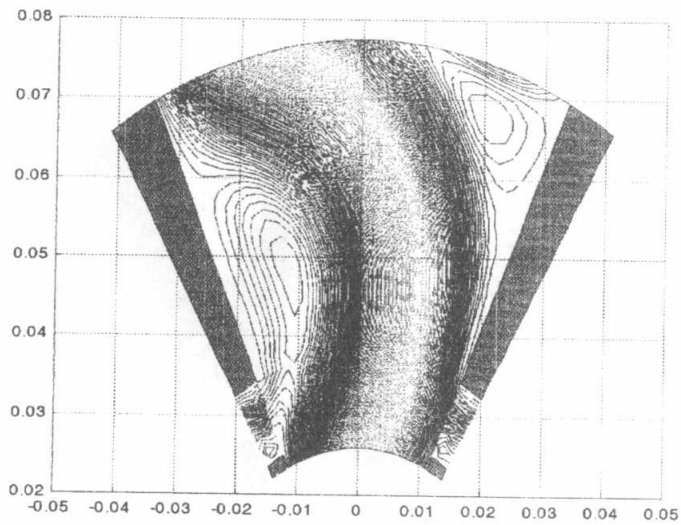


Fig.9. Streamlines of the slotted impeller using primitive variables approach. ( $Q=0.5Q_n=0.008104 \text{ m}^3/\text{s}$ ,  $L=0.01\text{m}$ ,  $R_s=0.035\text{m}$ , and  $H=7.8403\text{m}$ )

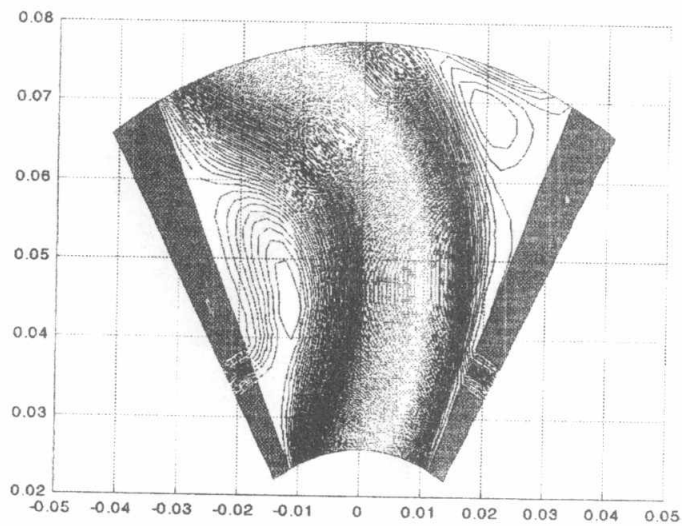


Fig.10. Streamlines of the slotted impeller using primitive variables approach. ( $Q=0.5Q_n=0.008104 \text{ m}^3/\text{s}$ ,  $L=0.0052\text{m}$ ,  $R_s=0.04\text{m}$ , and  $H=7.7978\text{m}$ )

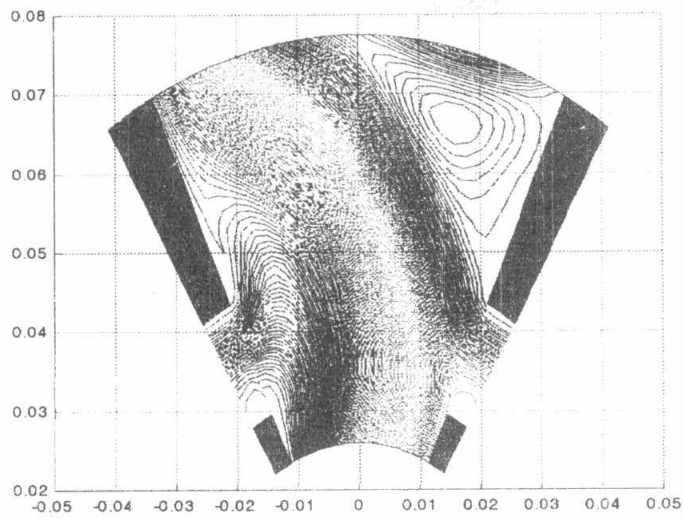


Fig.11. Streamlines of the slotted impeller using primitive variables approach.  
( $Q=0.5Q_n=0.008104 \text{ m}^3/\text{s}$ ,  $L=0.0155\text{m}$ ,  $R_s=0.04\text{m}$ , and  $H=9.417\text{m}$ )

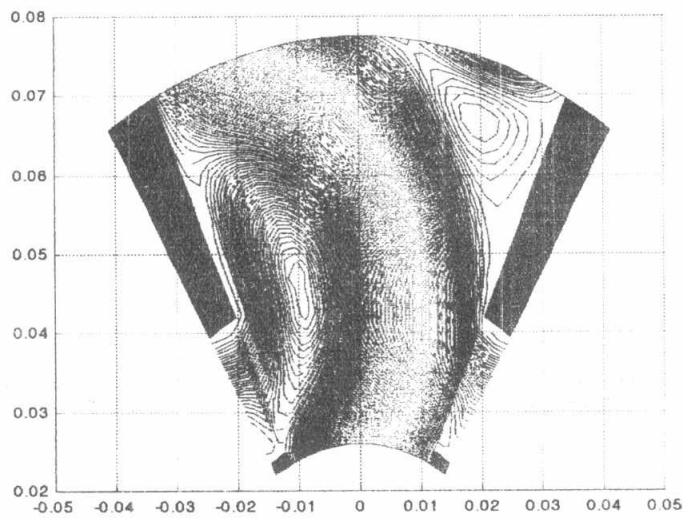


Fig.12. Streamlines of the slotted impeller using primitive variables approach.  
( $Q=0.5Q_n=0.008104 \text{ m}^3/\text{s}$ ,  $L=0.02\text{m}$ ,  $R_s=0.04\text{m}$ , and  $H=8.2559\text{m}$ )



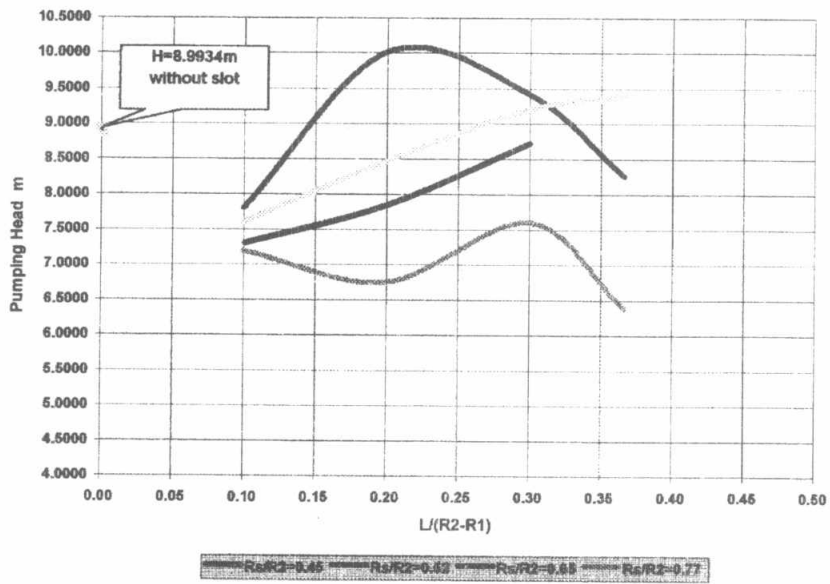


Fig.13. The pumping head versus  $R_s/R_2$  with fixed slot length ( $L/(R_2-R_1)=0.099$ ).

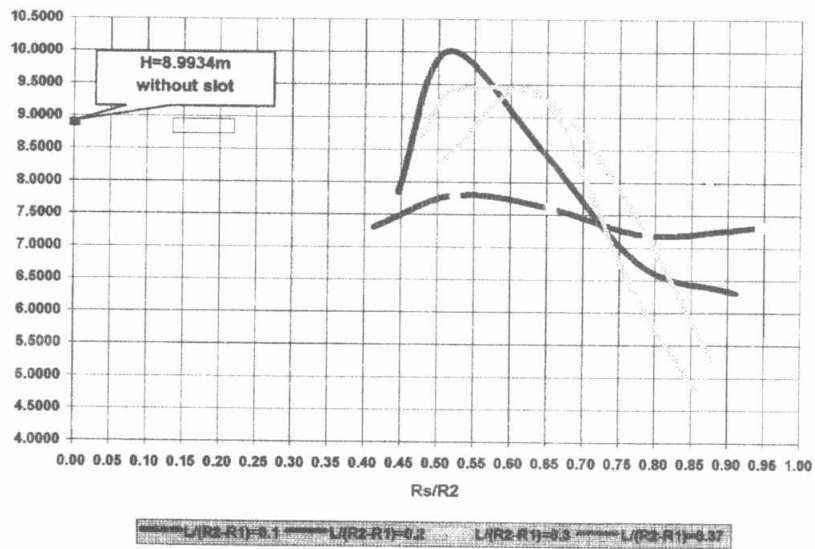


Fig.14. The pumping head versus  $L/(R_2-R_1)$  at fixed slot position ( $R_s/R_2=0.4981$ ).